MECSOL 2022 - Proceedings of the 8th International Symposium on Solid Mechanics
M.L. Bittencourt, J. Labaki, L.C.M. Vieira Jr. and E. Mesquita (Editors), Campinas SP, Brazil, October 17th to 19th, 2022

On the dependence of the initial yield stress on the stress triaxiality and the Lode parameter

Raphael Luís de Mecê Mialhe[1], Michael Brünig[2], Larissa Driemeier[1]

[1] University of São Paulo, Polytechnic School, Av. Prof Melo Moraes, 2231, Brazil

[2] Universität der Bundeswehr München, Institut für Mechanik und Statik, Germany

Abstract: For safety reasons, many structures are designed to work in elastic regime, making the material initial yield stress a critical value. Although there are many mathematical models available to describe the mechanical behavior of ductile materials, establishing mathematical relationships that weigh the influence of a complex stress state on the initial yield stress of the material is not a trivial task. In this context, the present work studies the influence of stress state on the onset of yield stress for different aluminum alloys through the numerical analyses of three different biaxial models. The experimental results for model training and validation were obtained from the literature. Firstly, the material parameters were determined by adjusting numerical and experimental force versus displacement curves. Then, finite element analyses were performed to extract stress invariants at the beginning of material yielding. Finally, a nonlinear regression was implemented to adjust the parameters of a polynomial to model the initial yield stress as a function of the stress triaxiality and Lode parameter. The results indicate that the yield stress behavior, for the tested range of triaxiality and Lode parameter values, can be robustly modelled by a fourth-order polynomial.

Keywords: biaxial experiments; yield criterion; stress state invariants; Lode angle; triaxiality; finite element analysis

INTRODUCTION

Although there are many mathematical models available to describe mechanical behavior of ductile materials, establishing theoretical mathematical relationships that ponder the influence of a complex stress state on material yield stress is not a trivial task. Hence, still nowadays, classical expressions that give reasonable results with few material parameters are used in practice as yield criteria. For example, Tresca and von Mises are well known yield stress criteria.

However, pioneer studies from Spitzig and Richmond (1984), Spitzig, Sober and Richmond (1975) and Spitzig, Sober and Richmond (1976) considered hydrostatic pressure as a contributing factor for material yielding. Moreover, there are more recent criteria proposed in literature that consider hydrostatic pressure and Lode angle as influential factors to yield stress in isotropic materials, such as: Bardet (1990); Bai (2008); Yang, Sun and Hu (2009); Gao et al. (2011); Yoon et al. (2014); Mirone, Barbagallo and Corallo (2016); Cazacu and Revil-Baudard (2016); Zhang et al. (2020), etc.

Yang, Sun and Hu (2009), for example, proposed a modified von Mises criterion with Lode dependence and reported that the yield behavior of 2A12-T4 specimens were affected by Lode parameter more than by hydrostatic pressure. Cazacu and Revil-Baudard (2016) related that, for a particular combination of stress invariants, there is no influence of the third invariant of deviatoric stress tensor on yielding of porous materials. Ma et al. (2017) reported that for the same stress triaxiality, the Lode parameter has an effect on yield of aluminum alloy AlSi9Mn at negative stress triaxiality. Zhang et al. (2020) developed a new yield criterion that varies linearly with the Lode parameter and has good accuracy with experimental data.

Peng, Zhao and Li (2021) proposed an uncoupled ductile fracture model, dependent on triaxiality and Lode parameter, resulting in fracture strain decrease with stress triaxiality increase, being consistent with experimental data.

This paper studies the influence of the stress state on the onset of yield through three different cruciform specimens, named Z, H and X, respectively obtained from Driemeier et al. (2010), Gerke, Adulyasak and Brünig (2017), Gerke *et al.* (2018). In this context, it was attempted to develop a relationship, obtained from computational approaches, between yield stress, stress triaxiality and Lode parameter. Experimental data were provided to train and validate the proposed model.

Stress state invariants

Any stress state for isotropic materials, as well as its yield condition, can always be expressed as a function of the stress invariants I_1, J_2 and J_3, shown in Eq. (1).

$$I_1 = \mathrm{tr}(\sigma_{ij}) = \sigma_1 + \sigma_2 + \sigma_3$$

$$J_2 = \frac{1}{2} s_{ij} s_{ij} = \frac{1}{6}[(s_1 - s_2)^2 + (s_2 - s_3)^2 + (s_3 - s_1)^2] \quad (1)$$

$$J_3 = \det(s_{ij}) = s_1 s_2 s_3$$

where σ_1 , σ_2 and σ_3 are the three principal stresses of Cauchy stress tensor, $\boldsymbol{\sigma}$, with $\sigma_1 > \sigma_2 > \sigma_3$. The stress tensor can be decomposed into two portions: a hydrostatic stress tensor, $\boldsymbol{\sigma_H}$, which governs volume changing of a stressed body and the stress deviator tensor, **s**, which contributes to body distortion, whose principal stresses are s_1, s_2 and s_3. Then, the stress tensor components, σ_{ij}, are expressed in Eq. (2).

$$\sigma_{ij} = s_{ij} + \sigma_H \delta_{ij} = s_{ij} + \frac{1}{3} I_1 \delta_{ij} \quad (2)$$

where s_{ij} is the stress deviator tensor components and δ_{ij} is the Kronecker delta.

Two parameters may represent these three invariants: stress triaxiality (η) and Lode parameter (μ). Both are respectively given by Eqs. (3) and (4).

$$\eta = \frac{\sigma_H}{q} = \frac{\sigma_1 + \sigma_2 + \sigma_3}{3} \quad (3)$$

$$\mu = \frac{2\sigma_2 - \sigma_1 - \sigma_3}{\sigma_1 - \sigma_3} \quad (4)$$

where q is the von Mises equivalent stress, given by Eq. (5).

$$q = \sqrt{3J_2} \quad (5)$$

Specimen geometries

Detailed information about the geometries of the biaxial specimens, designed with the purpose of covering a wide range of stress states, is given in Figs. 1, 2, and 3. The specimens were tested in a biaxial machine, and different stress states are obtained varying the applied monotonic force ratio. The force ratio is defined as the relation between F_1 (in X direction) and F_2 (in Y direction), as defined in the figures.

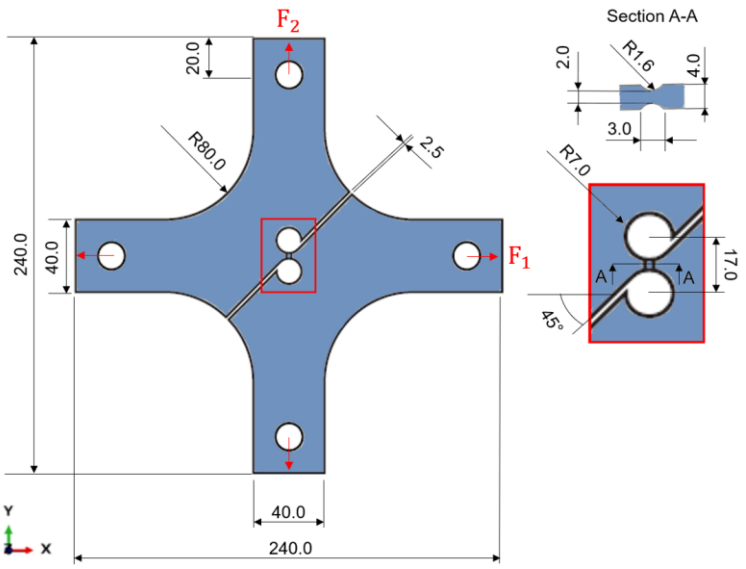

Figure 1 – Z specimen. Geometry design proposed in Driemeier et al. (2010)

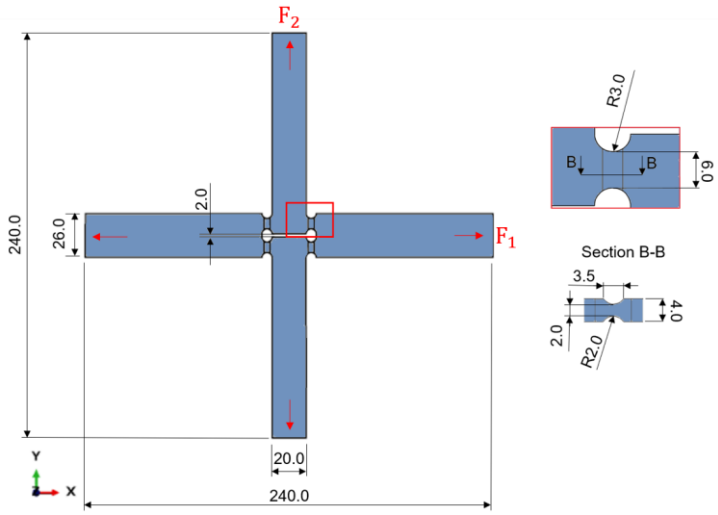

Figure 2 – H specimen. Geometry design proposed in Gerke, Adulyasak and Brünig (2017)

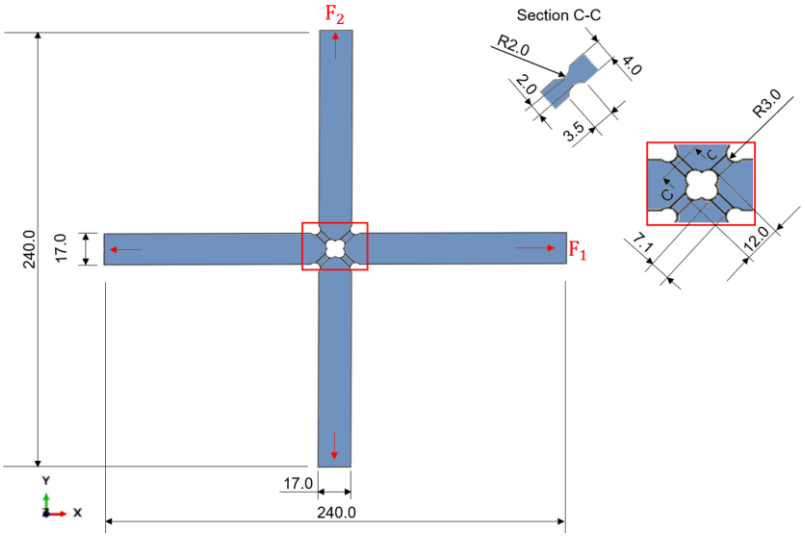

Figure 3 – X specimen. Geometry design proposed in Gerke et al. (2018)

Definition of material properties

The Z specimen parameters were determined based on results of uniaxial tests of a dog-bone shape specimen (Fig. 4) with thickness of 4 mm, flat and without notches.

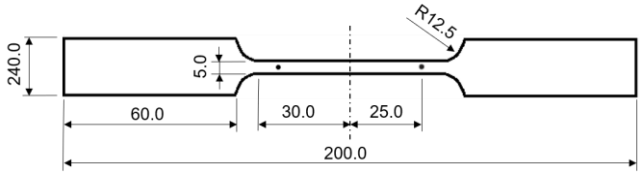

Figure 4 – Dimensions of dog-bone shape specimen

The obtained values for Young modulus and yield stress were, respectively, 68000 MPa and 250 MPa.

The material model of H and X specimens was made using Voce's Law, expressed in Eq. (6), according to Gerke, Adulyasak and Brünig (2017).

$$\sigma = \sigma_e + R_0 \varepsilon_p + R_\infty \left(1 - e^{-b\varepsilon_p}\right) \tag{6}$$

where R_0 and R_∞ are model coeficients and b is the hardening exponent. These are, respectively, equal to 680 MPa, 130 MPa and 30, to the considered alloys. σ is the current stress, ε_p is the plastic strain and the yield stress σ_e was initially set

to 300 MPa and was changed as required to adjust force versus displacement curves of H e X specimens. The Young modulus value that guarantees best curves adjustment to H specimen is 55 GPa, whereas, to X specimen, 68 GPa.

For all specimens, a Poisson coefficient equal to 0.3 and a density value of 2.78E-09 t/mm^3 were used.

The specimens with different loading ratios in the X and Y directions were numerically simulated, based on the work of Brünig, Gerke and Schmidt (2018). Different combinations of stresses were obtained, generating a wide range of values for each stress invariant. For Z specimen, the following loading relationships were used, respectively in the X and Y directions: -5:1, -6:1, -7:1. Regarding H specimen, the ratios used were: 0.5:1, -0.5:1, 1:1 and 3:1. For X specimen, the defined ratios were: 1:1, -0.5:1, -1:1, -2:1.

Tabs. 1, 2 and 3 show, respectively, the boundary conditions of Z, H and X specimens. The red marked spaces indicate that there was restriction of translational, rotational or both movements, for a given load ratio, in relation to the X, Y and/or Z axes.

Table 1 – Restrictions on degrees of freedom in Z specimen

Loading ratio	Node	Restrictions						
		Translation			Rotation			
		X	Y	Z	X	Y	Z	
All relationships	Top			■	■	■	■	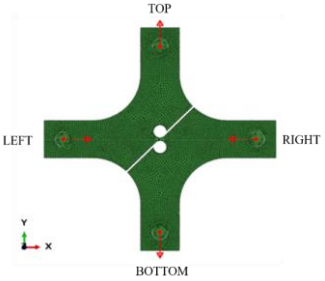
	Bottom			■	■	■	■	
	Right			■	■	■	■	
	Left			■	■	■	■	

Table 2 – Restrictions on degrees of freedom in H specimen~

Loading ratio	Node	Restrictions						
		Translation			Rotation			
		X	Y	Z	X	Y	Z	
All relationships	Top	■		■	■	■	■	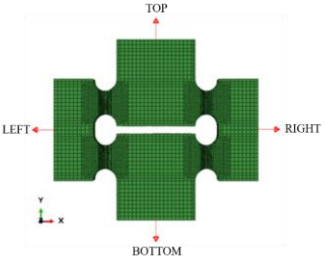
	Bottom	■		■	■	■	■	
	Right		■	■	■	■	■	
	Left		■	■	■	■	■	

Table 3 – Restrictions on degrees of freedom in X specimen

Loading ratio	Node	Restrictions						
		Translation			Rotation			
		X	Y	Z	X	Y	Z	
All relationships	Top			■	■	■	■	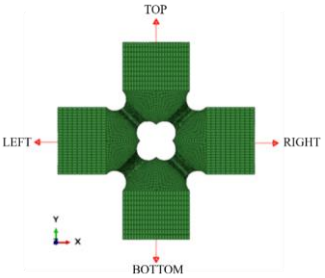
	Bottom			■	■	■	■	
	Right		■	■	■	■	■	
	Left		■	■	■	■	■	

The displacements measurement in the specimens during the experimental tests was performed with digital image correlation technique (DIC), using, as reference, the highlighted red points shown in Figs. 5, 6 and 7, corresponding to finite element mesh of specimens Z, H and X, respectively.

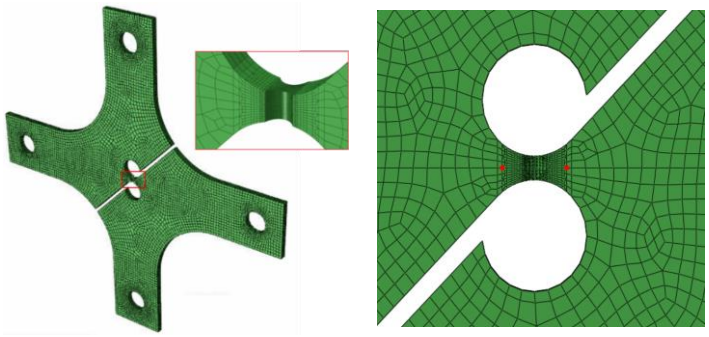

Figure 5 – DIC displacement measurement points on Z specimen

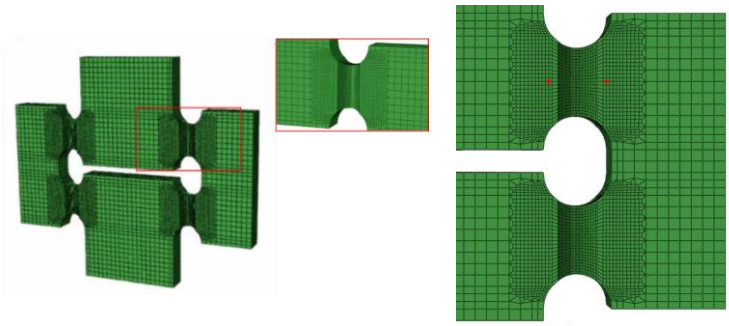

Figure 6 – DIC displacement measurement points on H specimen

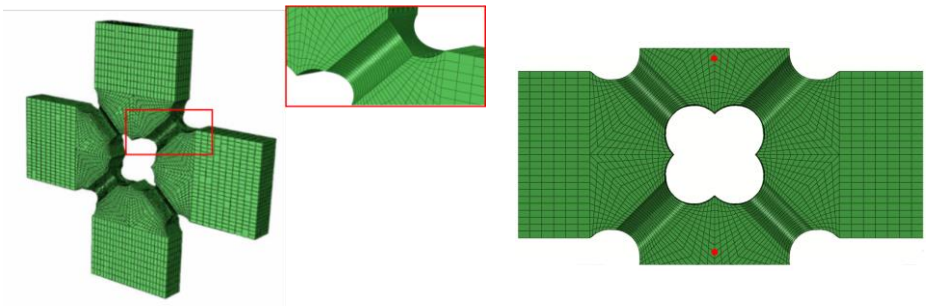

Figure 7 – DIC displacement measurement points on X specimen

Figure 8 depicts some experimental and numerical force versus displacement curves for Z, H and X specimens. Each specimen, tested with different load ratios, showed different behaviors. As the numerical curves overlapped the experimental ones by the red point, which indicates the onset of yield, triaxiality and Lode parameter were obtained in this area via numerical simulations.

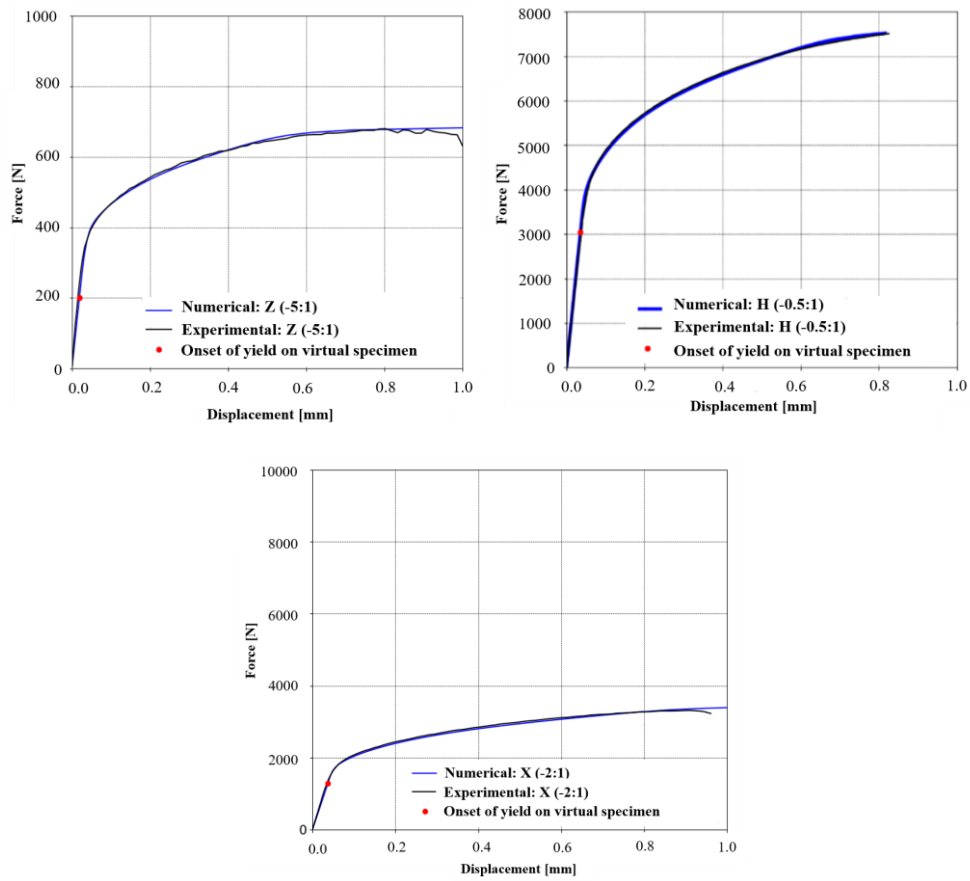

Figure 8 – Numerical and experimental force versus displacement curves

Results

To overcome the discrepancies due to different mechanical properties of the aluminum alloys, the normalized yield stress was analyzed, which corresponds to the ratio between the yield stresses that provided a better overlap of the numerical curves to the experimental ones, in all specimens, and those obtained in the uniaxial tensile tests.

Figure 9 illustrates the points obtained from numerical simulations of specimens Z, H and X, expressed in triaxiality, Lode parameter and normalized yield stress space.

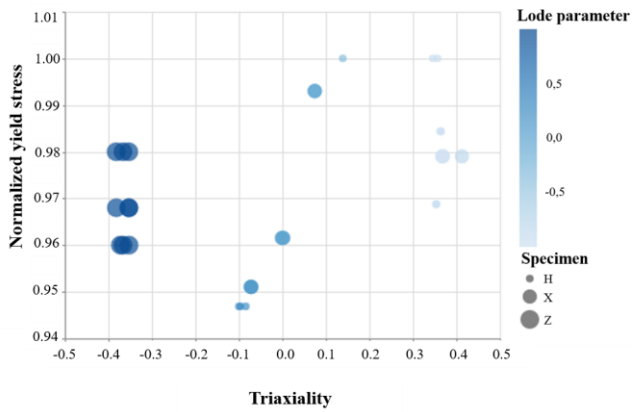

Figure 9 – Points obtained from finite element simulations

To perform surface adjustment to the observed points, a machine learning technique with cross validation was applied. Particularly, the Elastic Net regression model was used, adopting the triaxiality and the Lode parameter as independent variables and, as the dependent variable, the normalized yield stress. To verify the quality of surface fitting, coefficients of determination (R^2) were used with regard to prediction and generalization of the model.

The choice of the polynomial degree, the number of folds within cross-validation and the values of Elastic Net parameters α_{EN} and β_{EN} (Eqs. (7) and (8)) that provided the best result regarding the combination of coefficients of determination was carried out with the aid of a Python code that enabled the generation of different associations of these variables.

$$\alpha_{EN} = \lambda_{Ridge} + \lambda_{Lasso} \tag{7}$$

$$\beta_{EN} = \frac{\lambda_{Lasso}}{\lambda_{Ridge} + \lambda_{Lasso}} \tag{8}$$

where λ_{Ridge} and λ_{Lasso} are regularization coefficients of Ridge and Lasso regression models, respectively.

Figure 10 illustrates a flowchart which contains all steps taken to obtain the best surface fitting.

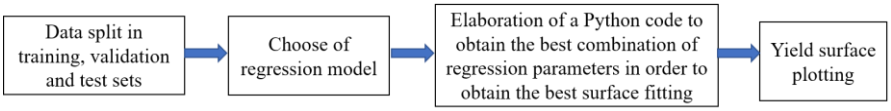

Figure 10 – Flowchart of yield surface achievement

The output showed that a fourth-degree polynomial regression model with low regularization (α_{EN}=0,0001), β_{EN}=0.2 and with a 2-fold cross validation presented the best result of surface fitting, with values of coefficients of determination for prediction and generalization equal to 0,79 and 0,57, respectively.

In addition to the small number of points obtained numerically, only 30% of these was used to compose the test data of the regression model. This may have resulted in the low value of the coefficient of determination for generalization. In this sense, the importance of carrying out more experimental tests with other force ratios is emphasized.

The yield surface is represented in different perspectives by Figs. 11, 12, 13 and 14.

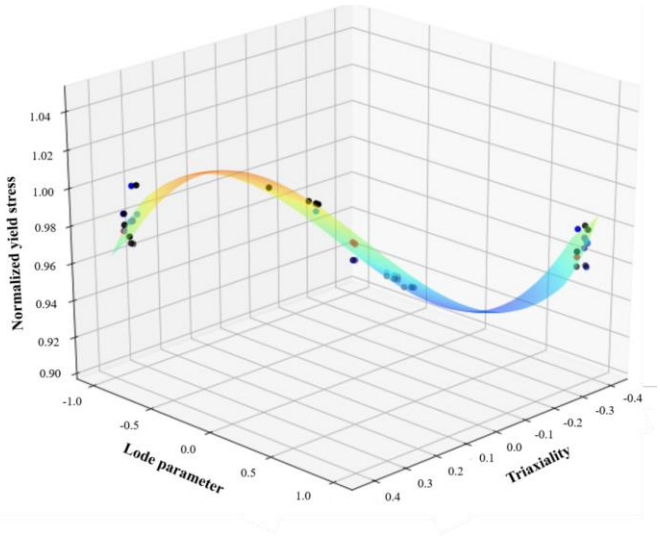

Figure 11 – Overview of the yield surface as a function of triaxiality and Lode parameter

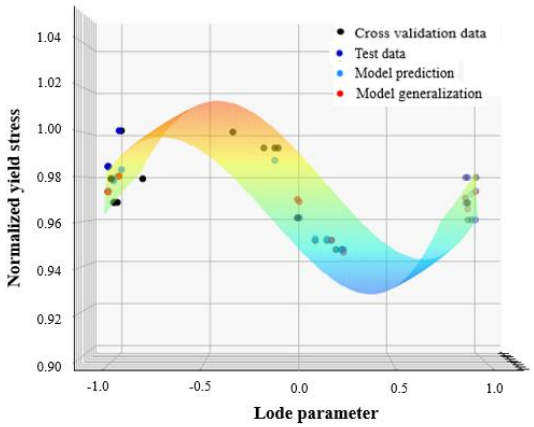

Figure 12 – Frontal view of the yield surface as a function of triaxiality and Lode parameter

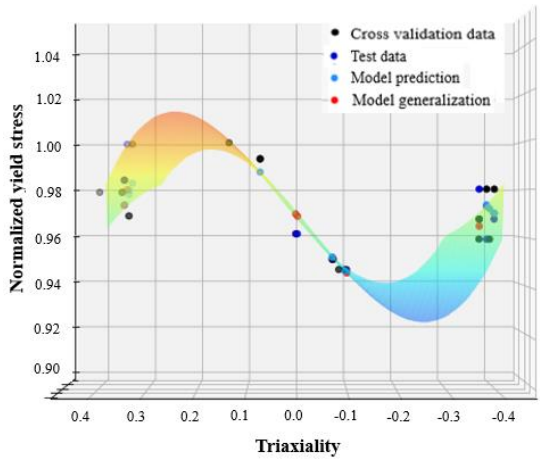

Figure 13 – Lateral view of the yield surface as a function of triaxiality and Lode parameter

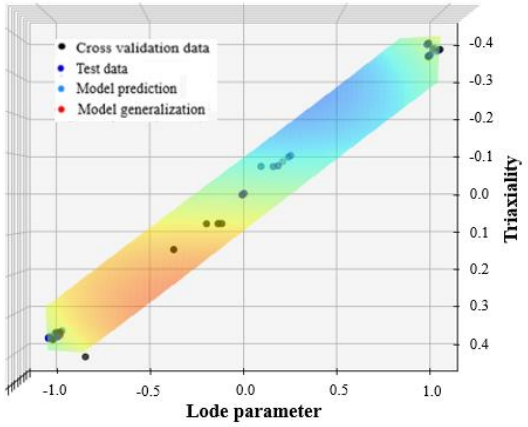

Figure 14 - Top view of the yield surface as a function of triaxiality and Lode parameter

According to Fig. 14, there is an approximately linear and inversely proportional relationship between triaxiality and Lode parameter. In fact, more points are required in regions that cover the ranges $0.18 < \eta < 0.35 \cup -0.9 < \mu < -0.4$ and $-0.35 < \eta < -0.12 \cup 0.3 < \mu < 0.9$. Thus, it is relevant to carry out more experimental and numerical tests covering these intervals.

By creating a cutting plane along the surface and projecting it on the frontal and lateral planes of the three-dimensional plot, Figs. 15 and 16 were obtained. These concern to, respectively, the variation of the normalized yield stress with triaxiality and with Lode parameter.

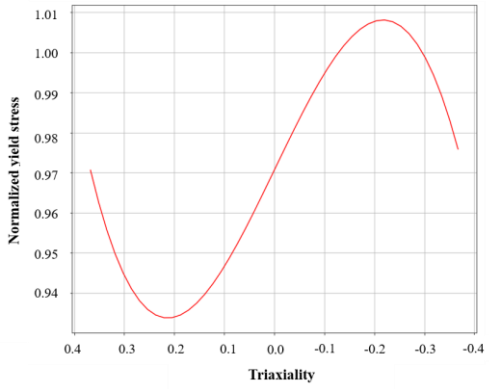

Figure 15 – Cross section view of the yield surface as a function of triaxiality

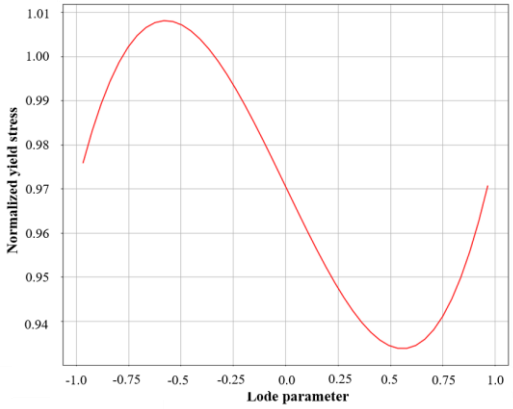

Figure 16 – Cross section view of the yield surface as a function of Lode parameter

It is observed that the behavior of the normalized yield stress, expressed as a function of the triaxiality and the Lode parameter, varies according to a specific range of values. In the triaxiality interval [-0.22, 0.22], the yield function increases, while outside this interval it decreases. Regarding the Lode parameter, in the interval [-0.60, 0.60], the behavior of the normalized yield stress decreases and, outside this interval, it increases. This yield surface is characterized by Eq. (9).

$$\sigma_{e_{norm}} = 0.97062053 + 0.2442346\eta - 0.00569165\mu - 0.86352576\eta^3 + 0.20757553\eta^2\mu - 0.03915723\mu^2\eta + 0.01029835\mu^3 + 0.14522556\eta^4 \quad (9)$$

It is important to note that this equation is valid only for the following domain: $-2.63\eta - 0.25 \leq \mu \leq -2.63\eta + 0.25$.

In contrast to what is reported in Yang, Sun and Hu (2009), as indicate the coefficients in Eq. (9), the Lode parameter exercised lower influence on the normalized yield stress behavior than triaxiality and, as opposed to what is related in Zhang et al. (2020), the obtained relationship between yield stress and Lode parameter is not linear. Furthermore, the largest coefficient associated only with the Lode parameter is approximately four times smaller than the smallest coefficient respective to a combination of the Lode parameter and triaxiality and ten times smaller than the smallest coefficient related only with triaxiality. Thus, it seems that the Lode parameter by itself did not exhibit significative influence on normalized yield stress.

Conclusions

It has been attempted to develop a numerical model to predict the occurence of plasticity for different aluminum alloys by means of a yield surface, expressed as a function of stress triaxiality and Lode parameter (μ).

Although no experimental tests were carried out, experimental results obtained from literature were used, which suited as a background to set material parameters in finite element models. From the overlap of the experimental force versus displacement curves to the numerical ones, the virtual models were considered coherent.

The specimen Z showed no significant variation of the invariants at the onset of yield. In this case, it would be interesting to carry out experimental tests of biaxial tension for a more in-depth analysis. Nevertheless, in the case of specimens H and X, it was found that the variation of the stress field during yielding provided a large range of triaxiality and, therefore, reinforces the importance of using specimens with different geometries, as shown in the literature.

The use of polynomial regression was essential to determine the influence of triaxiality and the Lode parameter on the normalized yield stress. The achieved mathematical relationship explains that the behavior of the normalized yield stress varies according to specific ranges of values of triaxiality and Lode parameter and does not coincide with some results presented in literature.

In accordance with the equation coefficients of the achieved yield surface, the Lode parameter by itself did not exhibit significative influence on the normalized yield stress compared to triaxiality or to the combination of Lode parameter and triaxiality.

Thus, it is suggested that further studies are conducted, considering other variables such as different geometries, materials and load combinations.

ACKNOWLEDGMENTS

The financial support of this work, provided by Coordenação de Aperfeiçoamento de Pessoal de Nível Superior (CAPES), is gratefully acknowledged.

REFERENCES

Bardet, J.P., 1990, “Lode dependences for isotropic pressure-sensitive elastoplastic materials”, Journal of Applied Mechanics, Vol.57, No. 3, pp. 498-506.

Bai, Y., 2008, “Effect of loading history on necking and fracture”, PhD Thesis – Massachusetts Institute of Technology.

Brünig, M.; Gerke, S.; Schmidt, M., 2018, “Damage and failure at negative stress triaxialities: experiments, modeling and numerical simulations”, International Journal of Plasticity, Vol.102, pp. 70-82.

Cazacu, O.; Revil-Baudard, B., 2016, “New analytic criterion for porous solids with pressure-insensitive matrix”, International Journal of Plasticity, Vol.89, pp. 66-84.

Driemeier, L.; Brünig, M.; Micheli, G.; Alves, M., 2010, “Experiments on stress-triaxiality dependence of material behavior of aluminum alloys”, Mechanics of Materials, Vol.42, No. 2, pp. 207-217.

Gao, X.; Zhang, T.; Zhou, J.; Graham, S. M.; Hayden, M.; Roe, C., 2011, “On stress-state dependent plasticity modeling: significance of the hydrostatic stress, the third invariant of stress deviator and the non-associated flow rule”, International Journal of Plasticity, Vol.27, No. 2, pp. 217-231.

Gerke, S.; Adulyasak, P.; Brünig, M., 2017, “New biaxially loaded specimens for the analysis of damage and fracture in sheet metals”, International Journal of Solids and Structures, Elsevier, Vol.110-111, pp. 209-218.

Gerke, S.; Zistl, M.; Schmidt, M.; Brünig, M., 2018, “Damage and fracture of ductile sheet metal: new biaxially loaded specimens for material parameter identification”, Procedia Structural Integrity, Vol.13, pp. 39-44.

Ma, Y.-S.; Sun, D.-Z.; Andrieux, F.; Zhang, K.-S., 2017, “Influences of initial porosity, stress triaxiality and Lode parameter on plastic deformation and ductile fracture”, Acta Mechanica Solida Sinica, Vol.30, No. 5, pp. 493-506.

Mirone, G.; Barbagallo, R.; Corallo, D., 2016, “A new yield criteria including the effect of Lode angle and stress triaxiality”, Procedia Structural Integrity, Vol.2, pp. 3684-3696.

Peng, Z.; Zhao, H.; Li, X., 2021, “New ductile fracture model for fracture prediction ranging from negative to high stress triaxiality”, International Journal of Plasticity, Vol.145, No. 6.

Spitzig, W.A.; Richmond, O., 1984, “The effect of pressure on the flow stress of metals”, Acta Metallurgica, Vol.32, No. 3, pp. 457-463.

Spitzig, W.A.; Sober, R. J.; Richmond, O., 1975, “Pressure dependence of yielding and associated volume expansion in tempered martensite”, Acta Metallurgica, Vol.23, pp. 885-893.

Spitzig, W.A.; Sober, R. J.; Richmond, O., 1976, “The effect of hydrostatic pressure on the deformation behavior of maraging and HY-80 steels and its implications for plasticity theory”, Metallurgical and Materials Transactions A, Vol.7, pp. 1703-1710.

Yang, F.; Sun, Q.; Hu, W., 2009, “Yield criterions of metal plasticity in different stress states”, Acta Matallurgica Sinica, Vol.22, No. 2, pp. 123-130.

Yoon, J.W.; Lou, Y.; Yoon, J.H.; Glazoff, M.V., 2014, “Asymmetric yield function based on the stress invariants for pressure sensitive metals”, International Journal of Plasticity, Vol.56, pp. 184-202.

Zhang, S.H.; Jiang, X.R.; Xiang, C.C.; Deng, L.; Li, Y.X., 2020, “Proposal and application of a new yield criterion for metal plastic deformation”, Archive of Applied Mechanics, Vol.90, No. 4, pp. 1705-1722.

RESPONSIBILITY NOTICE

The authors are the only parties responsible for the printed material included in this paper.